Supplementary Material Available: A table of anisotropic thermal parameters and a listing of the observed and calculated structure amplitudes (19 pages). Ordering information is given on any current masthead page.

References and Notes

(1) J. L. Little, G. D. Friesen, and L. J. Todd, *Inorg. Chem.*, **16**, 869 (1977).
(2) G. D. Friesen, A. Barriola, and L. J. Todd, *Chem. Ind. (London)*, 631 (1978).
(3) G. D. Friesen and L. J. Todd, *J. Chem. Soc., Chem. Commun.*, 349 (1978).
(4) V. D. Aftandilian, H. C. Miller, G. W. Parshall, and E. L. Muetterties, *Inorg. Chem.*, **1**, 734 (1962).
(5) E. I. Toplin and W. N. Lipscomb, *J. Am. Chem. Soc.*, **95**, 2384 (1973).
(6) J. C. Huffman, Ph.D. Thesis, Indiana University, Bloomington, IN, 1974.
(7) J. C. Huffman, C. R. Sporleder, and W. E. Streib, unpublished work.
(8) M. O. Visscher, J. C. Huffman, and W. E. Streib, *Inorg. Chem.*, **13**, 792 (1974).
(9) All computations were performed on a CYBER172-COC6600 computer using the I.U.M.S.C. XTEL interactive program library. The programs are based in part on A. C. Larson's Los Alamos code and J. A. Ibers' Northwestern University code.
(10) C. Tsai and W. Streib, *J. Am. Chem. Soc.*, **88**, 4513 (1966).
(11) G. Evrard, J. A. Ricci, I. Bernal, W. J. Evans, D. F. Dustin, and M. F. Hawthorne, *J. Chem. Soc., Chem. Commun.*, 234 (1974).
(12) F. R. Scholer and M. E. Leonowicz, unpublished results.
(13) E. L. Muetterties and W. H. Knoth, "Polyhedral Boranes", Marcel Dekker, New York, 1968, p 104.

Contribution from the Department of Chemistry,
Texas A&M University, College Station, Texas 77843

Palladium Tetraazaannulenes: Synthesis and Structure of Palladium 5,7,12,14-Tetramethyldibenzo[*b*,*i*][1,4,8,11]tetraaza[14]annulene

M. TSUTSUI,* R. L. BOBSEIN, G. CASH, and R. PETTERSEN

Received July 13, 1978

The first palladium dibenzotetraaza[14]annulenes have been prepared from the reaction of the free base ligand with bis(benzonitrile)palladous chloride. Analytical data are consistent with the proposed structures. Palladium 5,7,12,14-tetramethyldibenzo[*b*,*i*][1,4,8,11]tetraaza[14]annulene was characterized by single-crystal X-ray diffraction. The structure is monoclinic, space group $P2_1/n$, with a = 6.497 (2) Å, b = 18.652 (6) Å, c = 7.429 (3) Å, β = 104.44 (3)°, Z = 2, and mol wt 448.85. Data were collected using Mo Kα radiation (λ 0.710 69 Å) to a maximum 2θ of 50°. All the atoms, including hydrogen, were located on Patterson and Fourier maps and used in the refinement. The final discrepancy indexes were R_F = 3.6% and R_{wF} = 4.6% for 1013 independent reflections with $|F_o| \geq 3\sigma(F_o)$. The molecule has pseudoplanar geometry, a significant departure from other structures reported for this ligand.

Introduction

Palladium coordination complexes prefer a square-planar arrangement and are known to be among the most stable.[1,2] Ligands such as porphyrins, phthalocyanines, and tetraazaannulenes prefer to coordinate with a metal ion in a square-planar fashion. The fact that palladium porphyrins are very resistive to chemical demetalation illustrates the stability of palladium square-planar complexes.[3] Previous structural characterizations show that divalent metal ions coordinate with the 5,7,12,14-tetramethyldibenzo[*b*,*i*][1,4,8,11]tetraaza[14]annulene ligand in a square-pyrimidal arrangement.[4]

Dibenzotetraaza[14]annulene has been complexed with a variety of metals;[5-13] some of these complexes exhibit unusual geometries.[14-16] Metal tetraazaannulenes have been known to possess chemical and thermal stability as well as high catalytic activity, particularly as electrocatalysts.[17-19] A cobalt tetraaza[14]annulene has been used as the photoactive substituent in a potential solar energy storage system.[20]

To our knowledge, no one has reported a palladium complex of tetraaza[14]annulene. Although these macrocyclic ligands generally influence the physical and chemical properties of the metal,[21] an X-ray diffraction analysis of this first palladium tetramethyltetraazaannulene shows that palladium metal insertion has the effect of flattening a hitherto saddle-shaped ligand into a pseudoplanar configuration.[4,22,23]

Experimental Section

Bis(benzonitrile)palladous chloride[24] and 1,8-dihydro-5,7,12,14-tetramethyldibenzo[*b*,*i*][1,4,8,11]tetraaza[14]annulene (H_2TMTAA)[8] were mixed in refluxing benzene. The title compound, PdTMTAA, was obtained from the resulting precipitate. PdTMTAA crystallized as orange platelets in hexane. PdTMTAA decomposes at 150 °C to a yellow-brown compound, which melts at 260 °C. Anal.[25] Calcd. for Pd($C_{22}H_{22}N_4$): C, 58.87; H, 4.94; N, 12.48; Pd, 23.90. Found: C, 59.18; H, 5.12; N, 12.20; Pd, 23.51. The visible spectrum of PdTMTAA in dichloromethane has two peaks at 415 nm (log ϵ = 4.5) and at 490 nm (log ϵ = 4.2). The infrared spectrum of PdTMTAA in the solid phase (KBr) shows peaks at 1475, 1395, 1070, 820, and 790 cm^{-1}. The mass spectrum is consistent with the structure of PdTMTAA.[26] The parent ions around m/e 448 appear in an isotopic pattern typical of naturally occurring palladium.

Table I. Data Collection and Refinement Details for Pd($C_{22}H_{22}N_4$) (PdTMTAA)

diffractometer: Enraf-Nonius CAD-4[a]
monochromator: graphite crystal
radiation: Mo Kα (λ 0.710 69 A)
takeoff angle: 2.8°
scan speed: 4-20°/min
scan width: 1°
standards: 3
2θ limits of data: 50°

[a] Data taken by Molecular Structure Corp., College Station, TX 77840.

The palladium complex of 1,8-dihydrodibenzo[*b*,*i*][1,4,8,11]tetraaza[14]annulene (H_2TAA)[5] has also been prepared. The above complex, PdTAA, was synthesized in a manner similar to the previously described PdTMTAA synthesis. PdTAA was purified by sublimation. Anal.[25] Calcd. for Pd($C_{18}H_{14}N_4$): C, 55.05; H, 3.59; N, 14.26; Pd, 27.09. Found: C, 54.95; H, 3.59; N, 14.01; Pd, 27.56. The visible spectrum of PdTAA is a typical metal insertion spectrum with peaks at 363, 402, 424, 455, and 487 nm in chloroform. The spectrum is very similar to that of NiTAA[5] indicating that PdTAA is a planar molecule.[27]

Crystal Examination and Data Collection

All crystals of PdTMTAA examined were extremely thin plates, the large faces of which were parallelograms. The one selected for X-ray work measured 0.23 × 0.22 × 0.008 mm and was mounted with the fiber axis approximately parallel to the longest edges.

Data were collected by Molecular Structure Corp., College Station, TX. Details are presented in Table I. The following equations were used in reducing the data (Lp is the Lorentz-polarization factor, S is the scan rate, C is the total integrated peak count, B is the total background count, and R is the ratio of scan time to background counting time): $I = S(C - RB)$, $\sigma(I) = [S^2(C + R^2B) + 0.0025I^2]^{1/2}$,

Table II. Final Positional and Thermal Parameters of Nonhydrogen Atoms for $[Pd(C_{22}H_{22}N_4)]^a$

atom	x	y	z	U_{11}	U_{22}	U_{33}	U_{12}	U_{13}	U_{23}
Pd	0.0 (0)	0.0 (0)	0.0 (0)	0.0234 (3)	0.0250 (3)	0.0251 (3)	0.0002 (4)	0.0085 (2)	0.0005 (4)
N1	−0.0126 (8)	0.0563 (3)	0.2260 (7)	0.0221 (25)	0.0293 (27)	0.0268 (27)	0.0035 (21)	0.0053 (21)	−0.0026 (22)
N2	0.2027 (8)	0.0768 (3)	−0.0287 (7)	0.0277 (27)	0.0316 (27)	0.0269 (28)	0.0021 (23)	0.0092 (22)	0.0015 (23)
C1	0.1270 (10)	0.1144 (3)	0.2556 (9)	0.0253 (32)	0.0293 (32)	0.0311 (34)	−0.0020 (26)	0.0024 (26)	−0.0026 (27)
C2	0.1852 (11)	0.1578 (3)	0.4181 (10)	0.0350 (36)	0.0333 (35)	0.0325 (36)	0.0041 (30)	0.0073 (29)	0.0001 (30)
C3	0.3008 (12)	0.2194 (4)	0.4213 (11)	0.0422 (42)	0.0315 (35)	0.0438 (43)	0.0000 (32)	0.0017 (34)	−0.0123 (33)
C4	0.3619 (13)	0.2403 (4)	0.2642 (11)	0.0452 (44)	0.0247 (36)	0.0555 (51)	−0.0017 (33)	0.0073 (36)	0.0011 (34)
C5	0.3228 (11)	0.1972 (4)	0.1107 (11)	0.0283 (35)	0.0322 (36)	0.0442 (43)	0.0011 (28)	0.0112 (32)	0.0145 (32)
C6	0.2227 (9)	0.1302 (3)	0.1093 (9)	0.0223 (30)	0.0237 (30)	0.0336 (35)	0.0031 (25)	0.0058 (25)	0.0021 (26)
C7	0.3366 (10)	0.0675 (3)	−0.1382 (9)	0.0297 (34)	0.0287 (33)	0.0310 (34)	−0.0026 (27)	0.0128 (28)	0.0040 (28)
C8	0.3124 (11)	0.0116 (4)	−0.2650 (9)	0.0382 (34)	0.0368 (43)	0.0330 (32)	−0.0024 (33)	0.0200 (27)	0.0045 (32)
C9	0.1714 (10)	−0.0462 (3)	−0.3088 (9)	0.0290 (35)	0.0307 (34)	0.0256 (33)	0.0025 (28)	0.0063 (27)	0.0032 (26)
C10	0.5315 (11)	0.1123 (4)	−0.1240 (11)	0.0328 (38)	0.0396 (41)	0.0427 (43)	−0.0049 (33)	0.0150 (33)	0.0013 (35)
C11	0.2190 (13)	−0.0972 (4)	−0.4495 (12)	0.0405 (44)	0.0430 (45)	0.0474 (48)	−0.0027 (36)	0.0220 (36)	−0.0104 (37)

[a] The anisotropic parameters (Å^2) are used in the expression $\exp(-[2\pi^2(U_{11}h^2a^{*2} + U_{22}k^2b^{*2} + U_{33}l^2c^{*2} + 2U_{12}hka^*b^* + 2U_{13}hla^*c^* + 2U_{23}klb^*c^*)])$.

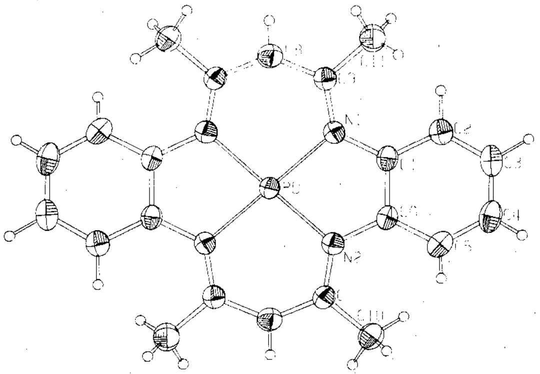

Figure 1. ORTEP of PdΓMTAA.

$|F_o| = (I/Lp)^{1/2}$, $\sigma(F_o) = \sigma(I)/2|F_o|Lp$. Periodic checks of three standard reflections revealed no deterioration during data collection. On the basis of ψ scans, absorption corrections were deemed unnecessary. The linear absorption coefficient, μ, is 10.65 cm^{-1}.

Solution and Refinement of the Structure

The structure was solved by use of the crystallographic multipurpose program SHELX (by George Sheldrick); thermal ellipsoid plots were generated by ORTEP (thermal ellipsoid plotting program by C. K. Johnson). These computations were performed on the Amdahl 470V/6 computer at Texas A&M University.

Systematic absences ($h0l$, $h + l \neq 2n$, and $0k0$, $k \neq 2n$) unambiguously identified the space group as $P2_1/n$. Since $Z = 2$, it was necessary that the palladium atoms lie on centers of symmetry. A Patterson map confirmed this. A difference Fourier synthesis revealed all the carbon and nitrogen atoms. Refinement of these, followed by a difference map, revealed all the hydrogen atoms also. When all the atoms had been refined to convergence (hydrogen atoms isotropic, others anisotropic), a difference map revealed no peak larger than 0.4 e/Å^3. The final unweighted R, defined as $\sum|F_o - |F_c||/\sum F_o$, was 0.036; the weighted R_w, $(\sum w|F_o - |F_c||^2/\sum wF_o^2)^{1/2}$, was 0.046. The weight, w, is given by $w = k/(\sigma^2(F_o) + gF_o^2)$; k was redetermined after each cycle, and g was refined at the same time by fitting $(F_o - F_c)^2$ to $(\sigma^2(F_o) + gF_o^2)/k$. The final values of k and g were 0.7731 and 8.93×10^{-4}, respectively. For the nonhydrogen atoms, the largest shift in a positional parameter on the last cycle was 0.35σ. Scattering factors used in these calculations were taken from ref 28. Cromer and Liberman's values[29] for the real and imaginary components of anomalous dispersion due to palladium were used.

Description and Discussion of the Structure of PdTMTAA

The final atomic coordinates are listed in Tables II and III. Listings of interatomic distances and bond angles are provided in Tables IV and V. Figure 1 is an ORTEP plot of PdTMTAA. This view of the structure is very similar to other published structures[4,7,21] in the general geometry of the ligand. The four Pd–N distances average 1.996 Å which is longer than the corresponding metal–nitrogen distances of 1.870 Å observed for NiTAA and 1.901 Å observed for CoTMTAAI. This

Table III. Final Positional and Thermal Parameters of Hydrogen Atoms for $[Pd(C_{22}H_{22}N_4)]$

atom	x	y	z	U, Å^2
H2	0.1357 (105)	0.1423 (34)	0.5310 (91)	0.0242 (174)
H3	0.3422 (109)	0.2473 (33)	0.5459 (98)	0.0387 (188)
H4	0.4361 (108)	0.2784 (36)	0.2651 (94)	0.0311 (186)
H5	0.3634 (117)	0.2116 (34)	0.0171 (100)	0.0343 (189)
H8	0.4211 (106)	0.0103 (31)	−0.3209 (87)	0.0278 (162)
H10A	0.4855 (111)	0.1547 (36)	−0.1947 (100)	0.0380 (203)
H10B	0.5854 (97)	0.1317 (34)	−0.0002 (92)	0.0251 (165)
H10C	0.6282 (118)	0.0820 (36)	−0.1737 (99)	0.0383 (198)
H11A	0.3605 (122)	−0.0892 (35)	−0.4464 (94)	0.0306 (184)
H11B	0.1355 (165)	−0.0896 (46)	−0.5826 (141)	0.0968 (311)
H11C	0.2096 (124)	−0.1430 (42)	−0.4123 (111)	0.0287 (239)

Table IV. Interatomic Distances in $[Pd(C_{22}H_{22}N_4)]$ (PdTMTAA), Å

Pd–N1	1.999 (5)	C1–C6	1.411 (9)
Pd–N2	1.993 (5)	C2–C3	1.370 (10)
Pd–C1	2.839 (6)	C3–C4	1.380 (11)
Pd–C6	2.840 (6)	C4–C5	1.366 (10)
C1–N1	1.395 (8)	C5–C6	1.408 (9)
C6–N2	1.413 (8)	C7–C8	1.388 (9)
C9–N1	1.340 (8)	C7–C10	1.498 (9)
C7–N2	1.342 (8)	C8–C9	1.400 (9)
C1–C2	1.424 (9)	C9–C11	1.502 (9)

Table V. Bond Angles for PdTMTAA, Deg

N2–Pd–N1	83.0 (2)	C5–C4–C3	120.4 (7)
C1–N1–Pd	112.3 (4)	C6–C5–C4	121.2 (7)
C6–N2–Pd	111.9 (4)	C1–C6–N2	115.7 (5)
C7–N2–Pd	121.2 (4)	C5–C6–N2	126.2 (6)
C7–N2–C6	125.1 (5)	C5–C6–C1	118.1 (6)
C2–C1–N1	126.8 (6)	C8–C7–N2	121.8 (6)
C6–C1–N1	115.8 (5)	C10–C7–N2	123.3 (6)
C6–C1–C2	117.4 (6)	C10–C7–C8	114.7 (6)
C3–C2–C1	121.3 (7)	C9–C8–C7	133.9 (6)
C4–C3–C2	119.7 (7)	C11–C9–C8	114.4 (6)

Table VI. Average N–M Distance for Various Macrocycles[a] and Empirical Crystal Ionic Radii of Metal Atoms,[b] Å

	distance	ionic radii
PdTMTAA	1.996	0.86
FeTMTAA	1.918	0.76
H_2TMTAA (N–H)	0.85	1.902 (N–Ct)
PdTPP	2.009	0.86
FeTPP	1.972	0.76
FeTPPCl	2.05	0.64
FePc	1.926	0.76
Fe(octaaza[14]annulene)	1.836	0.76
FeTMTAACl	2.002	0.64
CoTMTAAI	1.901	0.63
MnTMTAA·N(Et)$_3$	2.118	0.80
NiTAA	1.870	0.72
Ni$C_{20}H_{18}N_4$(NiDMTAA)	1.85	0.72

[a] References 7, 11, 21, and 30. [b] Reference 31.

Table VII. Average Bond Angles, deg,[a] Comparison of Average Dihedral Angles, deg,[a] and Selected Average Interatomic Distances, Å

	PdTMTAA	H_2TMTAA[a]	FeTMTAA[b]	MnTMTAA·$N(Et)_3$[c]	FeTMTAACl·CH_3CN[c]	CoTMTAAI·$CHCl_3$[c]	NiTAA[d]
α	133.9	127.3	129.9	131.2	129.6	130.2	124.1
β	122.1	120.1	121.6	123.1	121.5	121.4	124.7
γ	125.3	127.4	125.3	126.3	125.0	123.8	120.2
δ	115.7	117.3	114.0	115.6	113.9	113.2	113.6
1–2[a]	14.7	34.3	24.5	35.2	32.9	21.3	
1–3	1.4	20.1	17.5	12.4	16.3	16.2	
1–4	13.0	24.6	23.7	20.5	21.8	21.7	
5–6	25.0	45.6	31.5	51.3	43.5	28.5	
6–7	5.2	3.6	9.27	1.6	3.2	12.1	
av M–N dist	1.996		1.918	2.118	2.002	1.901	1.870
dist of M from N_4 donor plane	0.000	~0.1 (H's)	0.114	0.730	0.600	0.234	0.000
Ct–N dist	1.996	1.902		1.988	1.910	1.893	1.870
av C–N dist, six-membered chelate ring	1.341	1.330	1.342	1.327	1.331	1.344	1.327
av C–C dist, six-membered chelate ring	1.393	1.387	1.391	1.406	1.404	1.382	1.398
av C–N dist, five-membered chelate ring	1.404	1.404	1.418	1.403	1.422	1.411	1.418
d[a]	2.925	3.098	3.016	3.126	3.054	2.949	

[a] See Figure 3. [b] Reference 4. [c] Reference 11. [d] Reference 21.

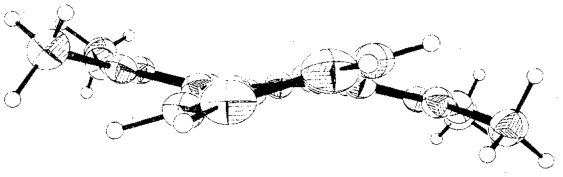

Figure 2. Side view of $Pd(C_{22}H_{22}N_4)$ illustrating deviations from the containing Pd and N's. (Space group symmetry requires that these five atoms be in the same plane.)

increase is expected because of the larger ionic radius of palladium. A comparison of M–N distances in various metallomacrocycles and crystal ionic radii of the metal atom is summarized in Table VI. The data in Table VI show that as the size of the metal increases, one expects a concomitant displacement of the metal from the N_4 plane or some kind of ligand distortion.[21] Possibilities for relieving ligand strain introduced by metal insertion include some combination of (1) an increase in interatomic distances on the 14-membered ring, (2) an increase in some of the interior angles of the ring, and (3) a deformation of the ring carbon atoms from the N_4 plane. As required by symmetry, the palladium atom in PdTMTAA does not deviate from the N_4 plane. The atoms of the 14-membered ring are displaced from the N_4 plane by a maximum of 0.467 Å, as illustrated in Figure 2. There are appreciable distortions in the five-membered chelate rings and in the benzenoid rings, but this pseudoplanar geometry contrasts with the very nonplanar geometry of other published TMTAA structures.[11,21] In the latter compounds, the methyl groups interact sterically with the benzenoid rings so as to warp or distort the ligand, thus relieving steric strain. It has been suggested that the size of the metal ion directly influences the degree of distortion.[11] In the case of PdTMTAA, the opposite effect is observed. The palladium complexation has flattened the normally saddle-shaped ligand H_2TMTAA.

The total angular change in the ten interior and four exterior angles as defined in Figure 3 is an important measure of the degree of expansion of the ring (see Table VII). The sum of the values of the ten interior and four exterior angles for H_2TMTAA, FeTMTAA, CoTMTAAI·$CHCl_3$, and FeTMTAACl·CH_3CN is smaller than the corresponding sum in PdTMTAA by 6.4, 16.8, 26.2, and 19.4°, respectively. Only MnTMTAA·$N(Et)_3$ shows a total angular expansion (2.2°)

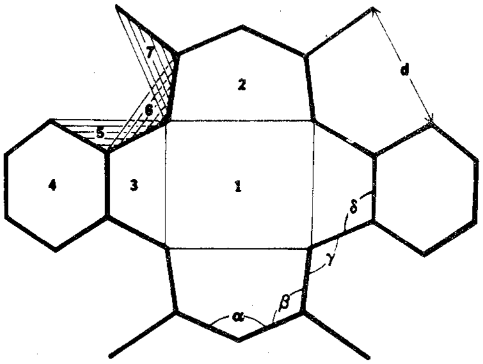

Figure 3. Definition of bond angles.[21]

compared with PdTMTAA. This similar total angular increase in the manganese compound does not permit the smaller manganese ion to sit in the N_4 plane. In this case the manganese ion also has a large axial ligand which may prevent the metal ion from sitting in the plane.

Since interatomic bond extensions are unlikely to occur because they are energetically unfavorable, it appears that ring expansion through increases in some interior bond angles provides most of the additional space required for the palladium ion to fit in. This factor probably influences the ability of the metal and the macrocycle to achieve the pseudoplanar configuration.

A comparison of some dihedral angles is also presented in Table VII. The dihedral angles as defined in Figure 3 are a measure of the distortion of the macrocyclic ligand. As can be seen from Table VII, TMTAA complexes of manganese, iron, and cobalt, as well as the free ligand, have a very large amount of distortion yielding the characteristic saddle shape. In contrast, PdTMTAA has, in general, about half the distortion. The dihedral angles between planes 1 and 3 (1.4°) and between planes 1 and 4 (13.0°) give an indication of the degree of deformation from planarity of the *o*-phenylenediamine moiety. The other compounds have much larger dihedral angles than those of PdTMTAA. Figure 2 illustrates the degree of deformation from planarity of the *o*-phenylenediamine moieties in PdTMTAA. The dihedral angle between planes 6 and 7 is larger for PdTMTAA than for H_2TMTAA, MnTMTAA·$N(Et)_3$, and FeTMTAACl·CH_3CN

and mainly indicates that the methyl group is displaced slightly out of the ligand plane. In fact, the nonbounding interactomic distance between the methyl group and the nearest carbon atom of the benenzoid ring for PdTMTAA is 2.925 Å, about 0.2 Å shorter than the corresponding distance in the manganese compound. Thus, in PdTMTAA there exists comparatively little warping of the macrocyclic ligand, and the methyl groups tilt slightly from the plane of the macrocycle as they get closer to the benzenoid rings. Table VII also presents a comparison of some selected bond lengths. The bond lengths of the PdTMTAA molecule are similar to those of some of the previously characterized TMTAA's. The average C–N distance in the six-membered ring in PdTMTAA shows more double bond character. The average C–C distance in the six-membered chelate rings is comparable in all seven compounds. The average C–N distance on the five-membered chelate ring shows more single bond character in all seven compounds.

Thus, it has been shown that palladium coordination to the TMTAA ligand yields a unique geometry. The strain generated by this pseudoplanar geometry is not alleviated by increased bond lengths or warping. Only the slight displacement of the methyl groups out of the plane and the angular increase may account for this planarity. Such an effect might be explained in terms of an especially strong palladium coordination sphere. In order to maximize such interactions, the tetramethyltetraazaannulene ring distorts from its usually stable saddle shape. First-row transition-metal complexes of the TMTAA ligand exhibit this saddle shape. Perhaps extended interactions by the larger palladium d orbitals force the ligand into its pseudoplanar configuration.

Acknowledgment. The authors acknowledge support of this research project by the Office of Naval Research and the Robert A. Welch Foundation.

Registry No. PdTMTAA, 68833-19-2; PdTAA, 68833-20-5; bis(benzonitrile)palladous chloride, 14220-64-5.

Supplementary Material Available: A listing of observed and calculated structure factors (5 pages). Ordering information is given on any current masthead page.

References and Notes

(1) F. A. Cotton and G. Wilkinson, "Advanced Inorganic Chemistry", Interscience, New York, 1972, p 1031.
(2) D. W. Thomas and A. E. Martell, *J. Am. Chem. Soc.*, **81**, 5111 (1959).
(3) V. Eisner and M. J. C. Harding, *J. Chem. Soc.*, 4089 (1964).
(4) V. L. Goedken, J. J. Pluth, S.-M. Peng, and B. Bursten, *J. Am. Chem. Soc.*, **98**, 8014 (1976).
(5) H. Hiller, P. Dimroth, and H. Pfitzner, *Justus Liebigs Ann. Chem.*, **717**, 137 (1968).
(6) E.-G. Jäger, *Z. Anorg. Allg. Chem.*, **364**, 177 (1969).
(7) F. Hanic, M. Handlovic, and O. Lindgren, *Collect. Czech. Chem. Commun.*, **37**, 2119 (1972).
(8) V. L. Goedken, J. Molin-Case, and Y.-A. Wang, *J. Chem. Soc., Chem. Commun.*, 337 (1973).
(9) V. L. Goedken and Y.-A. Park, *J. Chem. Soc., Chem. Commun.* 214 (1975).
(10) D. R. Neves and J. C. Dabrowiak, *Inorg. Chem.*, **15**, 129 (1976).
(11) M. C. Weiss, B. Bursten, S.-M. Peng, and V. L. Goedken, *J. Am. Chem. Soc.*, **98**, 8021 (1976).
(12) R. Müller and D. Wöhrle, *Makromol. Chem.*, **176**, 2775 (1975).
(13) R. Müller and D. Wöhrle, *Makromol. Chem.*, **177**, 2241 (1976).
(14) L. G. Bell and J. C. Dabrowiak, *J. Chem. Soc., Chem. Commun.*, 512 (1975).
(15) G. C. Gordon, P. W. Dehaven, M. C. Weiss, and V. L. Goedken, *J. Am. Chem. Soc.*, **100**, 1003 (1978).
(16) M. Tsutsui, R. L. Bobsein, R. Pettersen, and R. Haaker, submitted for publication.
(17) F. Beck, W. Dammert, J. Heiss, H. Miller, and R. Polster, *Z. Naturforsch.*, **28**, 1009 (1973).
(18) H. Alt, H. Binder, and G. Sandstede, *J. Catal.*, **28**, 8 (1973).
(19) F. Beck, *Ber. Bunsenges. Phys. Chem.*, **77**, 353 (1973).
(20) D. P. Fisher, V. Piermattie, and J. C. Dabrowiak, *J. Am. Chem. Soc.*, **99**, 2811 (1977).
(21) M. C. Weiss, G. Gordon, and V. L. Goedken, *Inorg. Chem.*, **16**, 305 (1977), and references cited therein.
(22) W. H. Woodruff, R. W. Pastor, and J. C. Dabrowiak, *J. Am. Chem. Soc.*, **98**, 7999 (1976).
(23) F. C. McElroy and J. C. Dabrowiak, *J. Am. Chem. Soc.*, **98**, 7112 (1976).
(24) M. S. Kharasch, R. C. Seyler, and F. R. Mayo, *J. Am. Chem. Soc.*, **60**, 882 (1938).
(25) Elemental analyses were performed by Schwarzkopf Microanalytical Laboratory, Woodside, NY 11377.
(26) Center for Trace Characterization, Texas A&M University, College Station, TX 77843.
(27) Infrared and mass spectral results are also consistent.
(28) "International Tables for X-ray Crystallography", Vol. 4, Kynoch Press, Birmingham, England, 1974.
(29) D. T. Cromer and D. Liberman, *J. Chem. Phys.*, **53**, 1891 (1970).
(30) E. B. Fleischer, C. K. Miller, and L. E. Webb, *J. Am. Chem. Soc.*, **86**, 2342 (1964).
(31) L. Pauling, "The Nature of the Chemical Bond", Cornell University Press, Ithaca, NY, 1960, p 518.

Contribution from the Department of Chemistry, Pacific Lutheran University, Tacoma, Washington 98447,
and the Chemical Physics Program, Washington State University, Pullman, Washington 99164

Crystal Structure and Magnetic Susceptibility of Di-μ-chloro-bis[chlorobis(tetramethylene sulfoxide)copper(II)], $Cu_2Cl_4(C_4H_8SO)_4$: An Antiferromagnetic Dimer

DUANE D. SWANK,* GREGORY F. NEEDHAM, and ROGER D. WILLETT

Received July 13, 1978

Crystals of $Cu_2Cl_4(C_4H_8SO)_4$ belong to the monoclinic space group $P2_1/c$ ($C_{2h}{}^5$) with lattice constants $a = 9.205$ (1) Å, $b = 14.614$ (9) Å, $c = 9.660$ (4) Å, $\beta = 84.629$ (3)°, $Z = 4$, $D_{\text{calcd}} = 1.76$ g/cm^3 and $D_{\text{measd}} = 1.77$ (2) g/cm^3. A room-temperature, single-crystal X-ray diffraction study was performed along with a study of the magnetic susceptibility from 4 up to 110 K. The structure was solved by direct methods and refined by full-matrix least-squares techniques to $R(F_o) = 0.049$ for 1544 unique reflections. The copper ion in each *trans*-$CuCl_2(C_4H_8SO)_2$ monomer has a significant tetrahedral distortion from planarity. Long Cu–Cl interactions between monomer units create discrete bibridged dimeric species. The copper–chlorine–copper bridging geometry is asymmetric with one long bond (3.020 Å) and one short bond (2.270 Å); the bridging angle is 88.5°. Magnetic susceptibility measurements over the temperature range 4–110 K show the salt is antiferromagnetically coupled ($J/k = -12$ K). Similarly, EPR measurements indicate weak interdimer interactions ($J'/k \approx 0.1$ K) also exist.

Introduction

Interest in the role of ligand characteristics such as size and geometry in determining magnetic interactions between metal ions has increased in recent years. The role of the ligand in determining bond angles and distances in bridging moieties and interchain exchange pathways lead to the investigation of a series of compounds of copper chloride with dimethyl sulfoxide ($(CH_3)_2SO$) and tetramethylene sulfoxide ((C-

---

*To whom correspondence should be addressed at Washington State University.

0020-1669/79/1318-0761$01.00/0